

On the unsteady loads induced by the bluff body wake of the Ariane 5 rocket.

Simon Marié* and Hadrien Lambaré†

Centre National d'Etudes Spatiales - Rond Point de l'Espace, Courcouronnes 91023 EVRY CEDEX, France
Tel:+33 1 60 87 71 14 e-mail: simon.marie@cnes.fr

1. Introduction

The rear-part of Ariane 5 rocket is the home of complex phenomena potentially involving loads on the main nozzle. In particular, during transonic flight, space launchers after-bodies are subjected to significant loads acting normally to the thrust. These dynamic loads are caused by fluctuating pressure induced by a massively detached and turbulent flow. Thus, knowledge and control of side loads are of primary importance for the mechanical design of the launcher. This problem is well known in the literature and a lot of studies has been experimentally [3, 2, 6, 9] and numerically [8, 7] investigated on axisymmetric step flows. The goal of this study is to present some results for the real Ariane 5 configuration. Recently, some wind-tunnel tests have been made on a 1/60 scaled model of the real Ariane 5 rocket for a deeper understanding of the phenomenon. This study presents a physical assessment of the wind-tunnel tests made on three different configurations. The results are principally obtained from unsteady kulites transducers. The role of geometrical parameters is highlighted and some discussions are made about the possibilities of reduction device.

2. Tests and Geometry

This work is based on the wind-tunnel tests made in NLR (Netherlands) [1, 4] in 2004 and will include the 2010 tests in the complete presentations. The most critical part of the geometry for side-loads considerations is located on the engine nozzle and the PTM (engine thermal protection). These parts have been instrumented with a total of 112 unsteady kulites distributed along 8 rings on a 1/60 scaled model of the real Ariane 5 rocket (Fig.1). For this study, we will consider the tests made for a Mach number of 0.8 with a null incidence ($\alpha = \beta = 0$). The fluctuating pressure is recorded during a period of 2.56 seconds sampled at $12800Hz$.

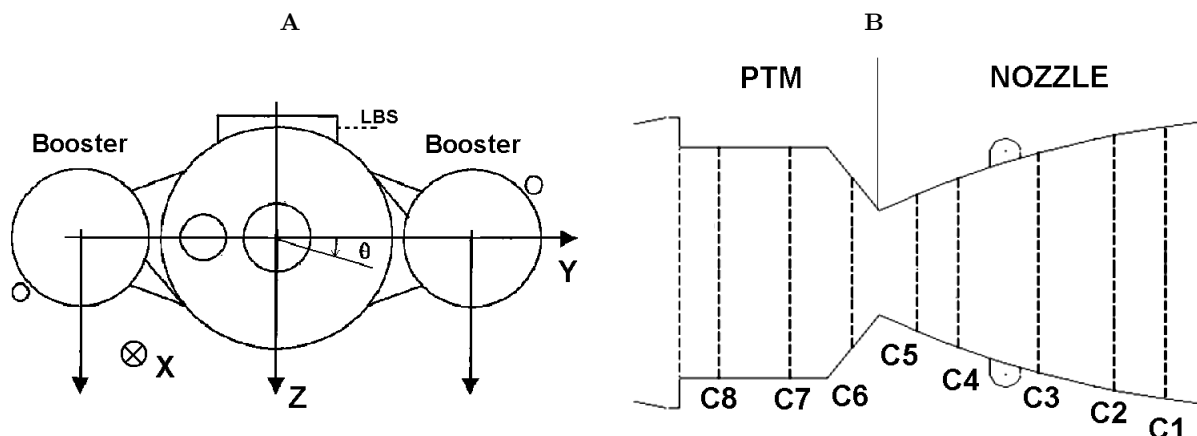


FIG 1. *A* Rear view of the geometry and principals axes of the model. *B* Position of sensors rings.

*Post-Doctoral student at CNES

†Expert engineer at CNES

In order to study the influence of the geometry, three different configurations will be investigated. The description of these configurations is shown on Fig.2.

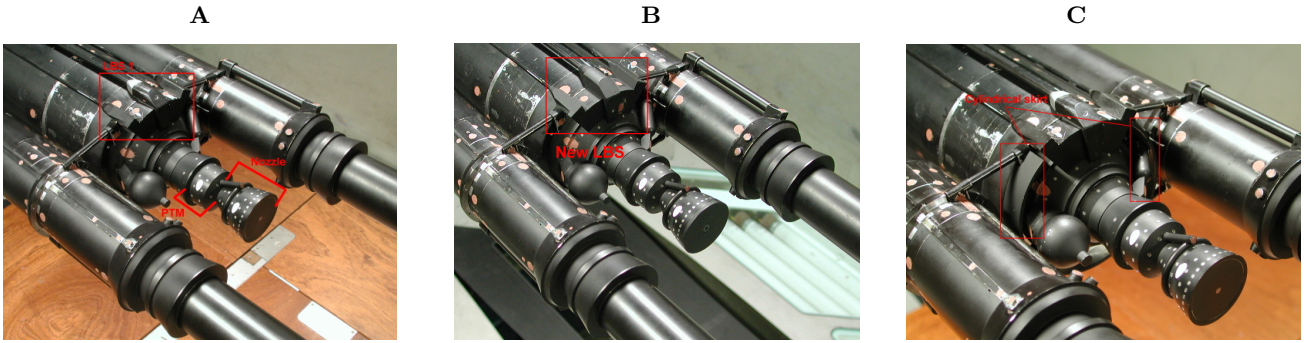


FIG 2. **A** Nominal configuration. **B** Configuration with a new LBS, **C** Configuration with a short cylindrical skirt.

These configurations are typical of three different flows inducing particular loads on the nozzle. The first configuration (Conf A) is the real model of the flying Ariane 5, the configuration with the new LBS (helium input for filling tanks at the ground) presents some minor geometrical modification inducing major consequences on the flow (Conf B) and the configuration with the skirt (Conf C) has been designed in order to reduce the loads.

3. Global approach

The first way to study the unsteady side-loads induced by the turbulent flow is to compute directly the global load acting on the nozzle. The direct experimental measurement of this quantity could be very difficult and demanding [3], therefore it could be useful to get this information from the kulites transducers by integrating the pressure along the nozzle:

$$\mathbf{F}(t) = \int_0^{2\pi} \int_0^L p(x, \phi, t) r(x) \mathbf{n} dx d\phi \equiv \sum_{i=1}^{N_c} p_i(t) d\mathbf{S}_i \quad (1)$$

The validity of such an integration depends on the number of sensors involved in the experimental process [5]. A simple way to check the integration validity is to observe the decay of the azimuthal modes obtained by the spatial Fourier series decomposition of the power spectral density (PSD) $G(\theta, f)$ of the fluctuating pressure along a ring:

$$\mathbf{G}(\theta, f) = a_0 + \sum_{m=1}^{\infty} \alpha_m(f) \cos m\theta + \beta_m(f) \sin m\theta \quad (2)$$

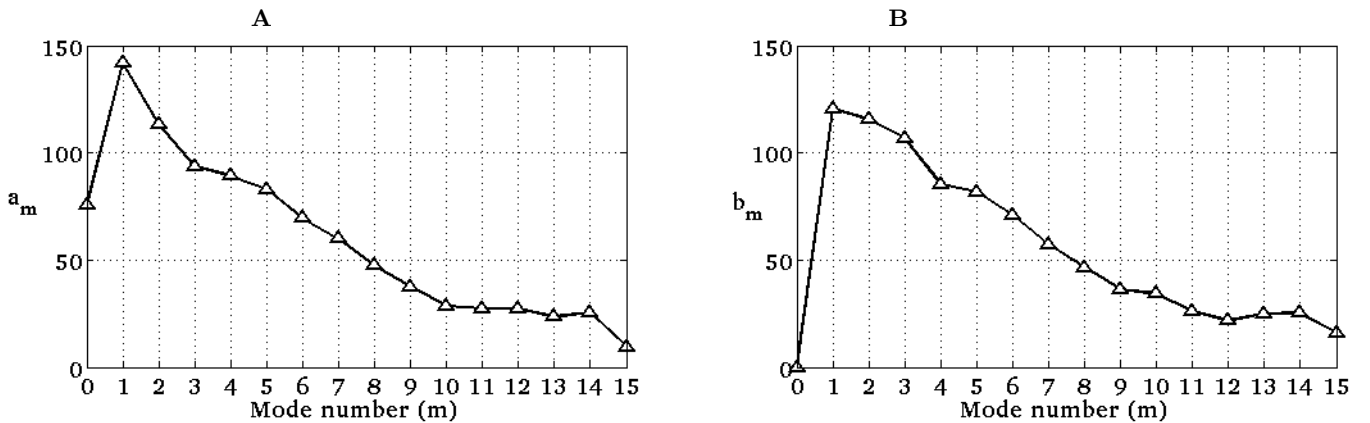


FIG 3. Amplitude of the azimuthal modes. **A** y-modes. **B** z-modes.

The mechanical response of the structure is characterised by a pendulum mode around 10Hz and an ovalisation mode around 25Hz. So the aerodynamic excitation should be evaluated around the same frequency range. With these considerations, let define $a_m = \int_{f_1}^{f_2} \alpha_m(f) df$ and $b_m = \int_{f_1}^{f_2} \beta_m(f) df$ with $f_1 = 5\text{Hz}$ and $f_2 = 40\text{Hz}$. The evolution of these coefficients is shown on Fig.3. The decrease of the mode amplitude allow us to use equation (1) to characterize the unsteady loads between 5 and 40Hz. The PSD of these loads is presented on Fig.4 for the three configurations.

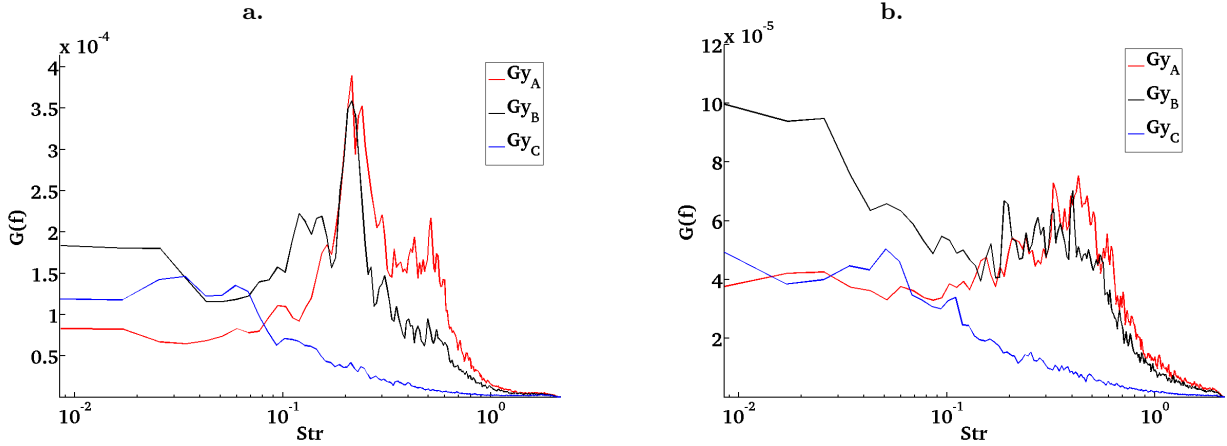


FIG 4. a. PSD of y-load induced by the $m = 1$ mode. b. PSD of y-load induced by the $m = 2$ mode. These curves are voluntarily set with arbitrary units

First, one can notice that the $m = 1$ mode excitation is characterized by a peak around $Str = 0.2$ ($= 10\text{Hz}$ at $\text{Mach} = 0.8$) and a broad-band load around $Str = 0.5$. Moreover, the $m = 2$ mode induces a broad-band load around $Str = 0.5$. This means that the aerodynamic excitation fits the mechanical response of the structure (pendulum mode and ovalisation mode). This explains why the phenomenon is so important and could be damaging for the launcher. Then, we observe that the new LBS (Conf B) induces some modifications in the unsteady load of the $m = 1$ mode around $Str = 0.5$. The local approach will allow us to deeper analyse these differences. Finally, we can note that the addition of a cylindrical skirt (Conf B) has a very positive effect on the phenomenon by reducing considerably the unsteady loads on the nozzle.

4. Local approach

An other way to study the buffeting phenomenon is to look at the pressure PSD repartition along the geometry of the rear-body. Let $G_p(\theta, x, f)$ be the pressure PSD at the point $[x, \theta]$. The quantity $f^*(\theta, x)$ such as:

$$G_p(\theta, x, f^*) = \max[G_p(\theta, x, f)] \quad (3)$$

is a way to study the local frequency behaviour of the phenomenon. Fig.5 represents $f^*(x, \theta)$ for the three configurations. The nominal configuration (Conf A) presents two particular areas ($25^\circ \leq \theta \leq 100^\circ$ and $220^\circ \leq \theta \leq 300^\circ$) where the maximal PSD are characterized by frequencies around 25Hz. This phenomenon could be interpreted as the consequences of the reattachment flow in these areas. Moreover, 10Hz frequencies ($Str = 0.2$ at $\text{Mach} = 0.8$) are observed in the overall geometry and are the signature of a global shedding phenomenon. Then, it is shown that the new LBS has a local effect on the pressure by suppressing the reattachment of the flow in the area $220^\circ \leq \theta \leq 300^\circ$. Finally, the addition of the cylindrical skirt suppresses the 25 Hz phenomenon and constitutes a good solution for unsteady load

reduction. Furthermore, we can show that an analysis of the pressure phases can link the local approach (pressure repartition) to the global approach (integrated load).

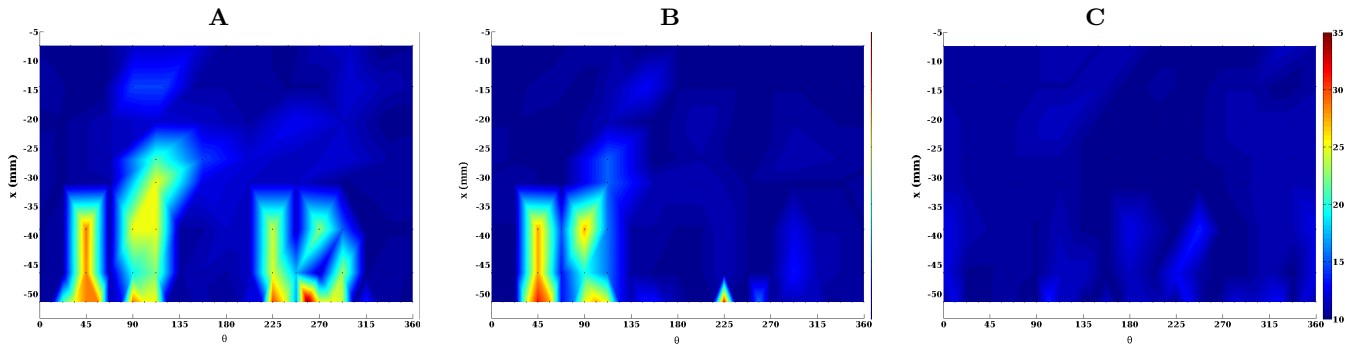


FIG 5. Frequency repartition of the maximal PSD along the nozzle and the PTM. Color scale refers to the frequency in Hz.

5. Conclusion

In this study, the experimental investigation of three geometrical configuration has been presented. An azimuthal mode decomposition has highlighted the repartition of the energy along the low level modes ($m = 1$ and $m = 2$) and the low frequencies. The analysis of the integrated load has revealed a peaked phenomenon around $str = 0.2$ associated with a broad-band load around $str = 0.5$. The local approach has identified these phenomenon as the signature of a shedding structure and a reattachment flow in the rear part of the nozzle. Finally, the reduction of the load induced by the addition of a skirt has been explained and it has been shown that small geometrical modifications (new LBS) could have significant impact on the flow. This later point will be further investigated during the planed 2010 wind tunnel tests.

References

- [1] DAVID, S. and RADULOVIC, S. (2005). Prediction of Buffet Loads on the Ariane 5 Afterbody. In *6th Symposium on Launcher Technologies*.
- [2] DUMNOV, G. (1996). Unsteady Side-Loads Acting on the Nozzle with Developed Separation Zone. *AIAA-paper 96-3220*.
- [3] GARÇON, F. and DREVET, J. (1998). Unsteady load measurements on the main engine nozzle of the Ariane 5 launch vehicle. In *Third European Symposium on Aerothermodynamics for Space Vehicles*. 623. ESA.
- [4] GEURTS, E. (2005). Steady and unsteady pressure measurements on the rear section of various configurations of the Ariane 5 launch vehicle. In *6th Symposium on Launcher Technologies*.
- [5] MARIÉ, S., DECK, S. and WEISS, P. (2009). From pressure fluctuations to dynamic loads on axisymmetric step flows with minimal number of kulites. *Accepted for publication in Computers & Fluids*.
- [6] MELIGA, P. and REIJASSE, P. (2007). Unsteady transonic flow behind an axisymmetric body equipped with two boosters. *AIAA paper 2007-4564*.
- [7] RAGAB, M. (1992). Buffet Loads Prediction for a Launch Vehicle and Comparison to Flight Data. *J. of Spacecraft and Rockets* **29**(6).
- [8] WEISS, P., DECK, S. and SAGAUT, P. (2008). Zonal-Detached-Eddy-Simulation of a Two-Dimensional and Axisymmetric Separating/Reattaching Flow. In *AIAA paper 2008-4377*.
- [9] WONG, H., MEIJER, J. and SCHWANE, R. (2007). Experimental and Theoretical Investigation of Base-Flow Buffeting on Ariane 5 Launch Vehicles. *J. Prop. and Power* **23**(1) 116-122.